

# Pendulum model approach to the dynamics of a Bose-Einstein condensate in a parabolic lattice

Joachim Brand<sup>1</sup> and Andrey R. Kolovsky<sup>1,2</sup>

<sup>1</sup> *Max-Planck-Institut für Physik komplexer Systeme, D-01187 Dresden, Germany and*

<sup>2</sup> *Kirensky Institute of Physics, 660036 Krasnoyarsk, Russia*

(Dated: May 23, 2019)

The dynamics of a Bose-Einstein condensate is studied in a combined periodic plus harmonic external potential. Unexpected regimes of stable collective dipole and Bloch oscillations are identified and explained in terms of quantum mechanical and classical pendulum models. The theoretical analysis is supported by full numerical solutions of the discrete and continuous nonlinear Schrödinger equation.

PACS numbers: 03.75.Lm, 05.45.-a

Recently much attention has been devoted to the properties of Bose-Einstein condensates (BECs) loaded into optical lattices [1, 2, 3, 4, 5, 6, 7, 8, 9, 10, 11, 12]. Indeed, this problem merges the field of Bloch theory with possible applications in the high-precision measurement of acceleration forces, with the field of nonlinear coherent waves with superfluidity and Josephson tunneling. Newly discussed effects include nonlinear Bloch waves [2, 3], nonlinear Landau-Zener tunneling [3, 4, 5], gap solitons [6, 7] and the disruption of Bloch oscillations [8, 9, 10, 11, 12].

When testing these newly predicted phenomena in laboratory experiments, an additional complication comes from the harmonic confinement, which can be stronger or weaker, but can never be avoided completely. In fact, it can introduce new effects. The dynamics of a BEC in a combined periodic plus parabolic potential was theoretically addressed in Refs. [13, 14, 15, 16, 17] (see also the single-atom analysis in Refs. [18, 19]) and is also a subject of this work. In Ref. [15] it was predicted that a BEC displaced from its equilibrium position in the trapping potential should undergo coherent oscillations for small displacements while, beyond a critical displacement, the BEC is pinned to the slope of the potential and relative phases are scrambled. This effect was interpreted as a dynamical superfluid-insulator transition and subsequently observed experimentally [11] and modeled numerically [17].

In this Letter we reinterpret the observed effect by mapping the physical system of a BEC in a parabolic lattice to a quantum mechanical pendulum model. The observed small-amplitude oscillations are the vibrations of the pendulum while large displacement may lead to pendulum rotations. The critical displacement observed is a manifestation of the classical separatrix separating vibrations and rotations. Contrary to the previous theoretical analyses [15, 16, 17] we find that a moderate repulsive nonlinearity may help to stabilize the wave-packet motion *below and above* the separatrix. Stabilization is accomplished by a cancellation of the wave-packet dephasing by the nonlinearity and classical pendulum motion is recovered below and well above the separatrix.

Assuming a deep optical lattice and using the tight-binding approximation,  $\psi(\mathbf{r}, t) = \sum_l a_l(t) \psi_l(\mathbf{r})$ , where

$\psi_l(\mathbf{r})$  are the localized Wannier states, the BEC dynamics is governed by the discrete nonlinear Schrödinger equation (DNLS),

$$i\hbar\dot{a}_l = \frac{\nu}{2}l^2a_l - \frac{J}{2}(a_{l+1} + a_{l-1}) + g|a_l|^2a_l, \quad (1)$$

where  $\nu$  is determined by the frequency  $\omega$  of the harmonic confinement,  $\nu = M\omega^2d^2$ ,  $d$  is the lattice period, and  $M$  the atomic mass. The hopping matrix element  $J \approx 8s^{3/4} \exp(-2\sqrt{s})/\sqrt{\pi}$  is uniquely defined by the depth of the optical lattice  $s = V_0/E_R$  measured in the units of the recoil energy  $E_R = 2\hbar^2\pi^2/d^2M$  and  $g$  is the interaction constant  $g = (4\pi\hbar^2a_s/M)N \int |\psi_l(\mathbf{r})|^4 d\mathbf{r}$ , where  $a_s$  is the  $s$ -wave scattering length and  $N$  the total number of atoms. Although the system (1) is usually discussed in terms of the Bloch states, one can obtain a more transparent description of its dynamics by mapping it to the mathematical pendulum [20]. Indeed, considering for the moment the linear case  $g = 0$  and introducing the function  $\phi(\theta, t) = 1/\sqrt{2\pi} \sum_l a_l(t) \exp(il\theta)$ , the system of equations (1) reduces to the Schrödinger equation for the quantum pendulum with the Hamiltonian

$$\hat{H} = \frac{\nu}{2}\hat{L}^2 - J \cos(\theta), \quad \hat{L} = -i\frac{\partial}{\partial\theta}. \quad (2)$$

A characteristic feature of the classical pendulum is the existence of a particular trajectory – the separatrix, which separates the vibrational and rotational regimes of the pendulum. This notion of the separatrix can be well extended into the quantum case [21]. It is associated with the critical angular momentum (or the critical site index of the original problem)

$$l^* = 2(J/\nu)^{1/2}. \quad (3)$$

As mentioned above, the existence of the critical  $l^*$  has been recently confirmed in the laboratory experiment [11], where the authors excite the system by suddenly shifting the harmonic trap by a distance  $\Delta x$ . Then, for  $l_0 = \Delta x/d < l^*$  (for the lattice parameters used in the cited experiment  $l^* = 134$ ) the wave packet oscillates around the trap origin, while for  $l_0 > l^*$  it sticks to one side of the parabolic potential. For  $g = 0$  these dynamical regimes are illustrated in Fig. 1, where the left and

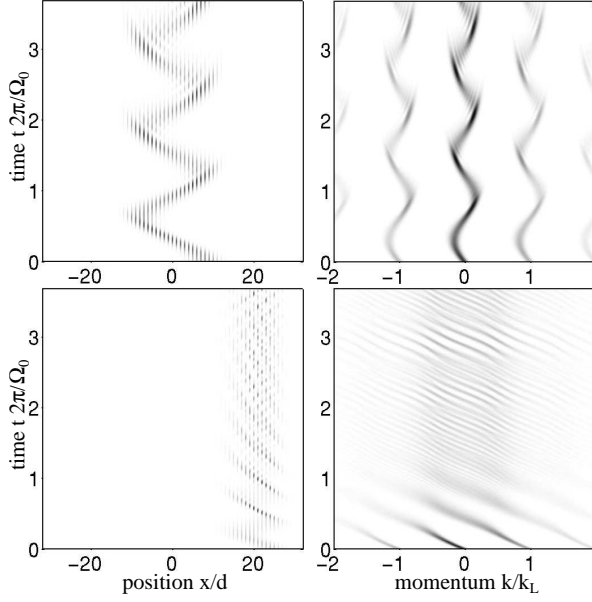


FIG. 1: Time-dependent density of a non-interacting atomic wavepacket ( $g = 0$ ) in greyscale in the real (left column) and momentum (right column) space. The system parameters corresponds to  $J = 2.4 \cdot 10^{-2} E_R$ ,  $\nu = 3.2 \cdot 10^{-4} E_R$  (hence,  $l^* = 17$ ) and initial shifts  $\Delta x/d = 8$  (upper row) and  $\Delta x/d = 24$  (lower row). The time axis is scaled by the period  $2\pi/\Omega_0$  of small-amplitude pendulum oscillations. Momentum is scaled by the reciprocal lattice constant  $k_L = 2\pi/d$ .

right panels corresponds to the coordinate and momentum representations, respectively. The characteristic frequency of the wave-packet oscillation is given by the pendulum frequency  $\Omega(l)$  [22]. Below the separatrix ( $l \ll l^*$ ) we have  $\Omega(l) \approx \Omega_0 = (\nu J)^{1/2} = \omega(M/M^*)^{1/2}$ , where  $M^*$  is the effective mass of an atom in the lowest Bloch band. At the separatrix  $\Omega(l^*) = 0$  and above ( $l \gg l^*$ ) we have  $\Omega(l) \approx \nu l$ . We note that Fig. 1 (and Fig. 2 below) show results obtained by using the continuous Schrödinger equation with a lattice depth of  $s = 12.16$ . The results obtained within the DNLS approach (not shown) practically coincide with the depicted ones.

In addition to the effect of the separatrix one can also see dephasing in Fig. 1, which smears out the oscillations of the wave packet as time goes on. This is a quantum-mechanical effect that can be related to the non-equidistant spectrum of the quantum pendulum. If  $l^* \gg 1$ , a short-time description of the dephasing can be obtained by solving the equations of motion of the classical pendulum for an *ensemble of trajectories* with initial conditions scattered over the phase volume  $\sim 2\pi\hbar_{\text{eff}}$  with  $\hbar_{\text{eff}} = (\nu/J)^{1/2} = 2/l^*$ . As a result we obtain a  $t^2$ -exponential decay for the oscillations of the mean coordinate and momentum of the atoms as shown in the upper panels of Fig. 4 and Fig. 5. (In comparison with Fig. 1, in Fig. 4 and Fig. 5 we decrease the trapping frequency so that the position of the separatrix (3) corresponds to  $l^* = 40$ . Also we used the DNLS instead of continuous Schrödinger equation to simulate the system

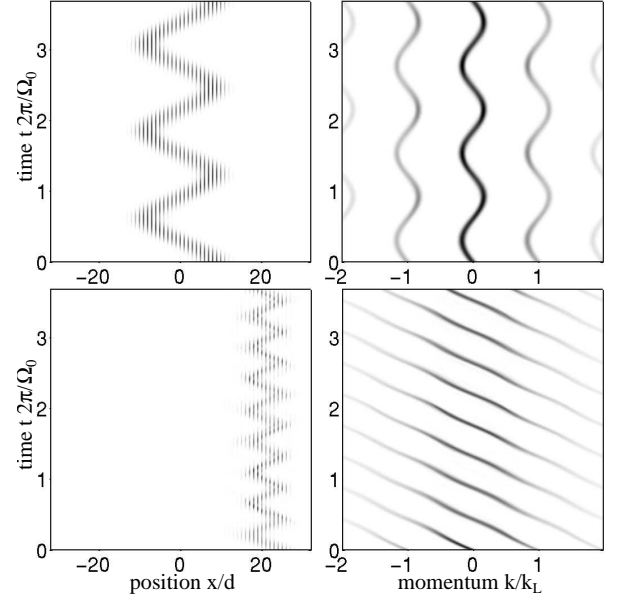


FIG. 2: The same as in Fig. 1 but for finite nonlinearity  $g = 1.55 \cdot 10^{-2} E_R$ .

dynamics.)

The main result we want to report in this letter is that a weak nonlinearity can compensate the dephasing, thus recovering the classical dynamics of the pendulum. This is illustrated in Fig. 2 and in the middle panels of Fig. 4 and Fig. 5.

In order to estimate the amount of nonlinearity required to convert the quantum dynamics of the pendulum into the classical dynamics, we use the Gaussian variational ansatz of Ref. [23]. For the quantum pendulum this amounts to a semiclassical approximation that can account for dephasing [24]. In this approach, the wave packet is parametrised as

$$a_l(t) = \sqrt{A} \exp \left[ -\frac{(l-L)^2}{\gamma^2} + i\theta(l-L) + i\frac{\delta}{2}(l-L)^2 \right], \quad (4)$$

where  $A$  is a normalization constant. Then the center of the wave packet  $L(t)$ , the dispersion  $\gamma(t)$ , the velocity  $\theta(t)$ , and the dephasing parameter  $\delta(t)$  satisfy Hamilton's equations for the effective Hamiltonian

$$H_{\text{eff}} = \frac{\nu}{2} \left( L^2 + \frac{\gamma^2}{4} \right) - J \cos \theta e^{-\eta} + \frac{g}{2\sqrt{\pi}\gamma}, \quad (5)$$

where  $\eta = 1/2\gamma^2 + \gamma^2\delta^2/8$  and the pairs of canonical variables are  $(L, \theta)$  and  $(\gamma^2/8, \delta)$ , respectively. Thus we have

$$\dot{L} = -J \sin \theta e^{-\eta}, \quad \dot{\theta} = \nu L, \quad (6)$$

$$\dot{\gamma} = J\gamma\delta \cos \theta e^{-\eta}, \quad \dot{\delta} = J \cos \theta \left( \frac{4}{\gamma^4} - \delta^2 \right) e^{-\eta} + \frac{2g}{\sqrt{\pi}\gamma^3} - \nu. \quad (7)$$

The non-dispersive dynamics of the wave packet depicted in Fig. 2 implies the (quasi)periodic dynamics of the variables  $L$ ,  $\theta$ ,  $\gamma$  and  $\delta$ . In fact, for the certain range of the nonlinearity  $g$  and harmonic confinement  $\nu$ , there is a stable periodic orbit in the four-dimensional phase space of the system (5), which comes through the point  $\delta = 0$ . The condition of existence of this periodic orbit is approximately given by the condition

$$g = \sqrt{\pi\nu}\gamma^3/2, \quad (8)$$

which means that the last two terms in the equation for  $\delta$  cancel each other. The examples of the discussed stable periodic orbits are shown in Fig. 3(a,b) for the parameters of Fig. 4(b) and Fig. 5(b), respectively. Additionally we depict in Fig. 3 the stability regions of the orbit together with the estimate (8). The bright regions correspond to the quasiperiodic dynamics with small deviations of  $\delta$  and  $\gamma$ . In the grey (red) regions the deviations are large and in the dark (blue) regions the dephasing  $\delta$  increases without bounds. It is worth of noting that the variational ansatz (4) becomes invalid as soon as the orbit is unbounded or badly bounded. On the other hand, if  $\delta(t)$  is captured around  $\delta = 0$  and  $\gamma$  is not too small as it occurs near the center of the stability island, we have  $\exp[-\eta(t)] \approx 1$  and Eq. (6) reduces to the equation of motion for a classical pendulum.

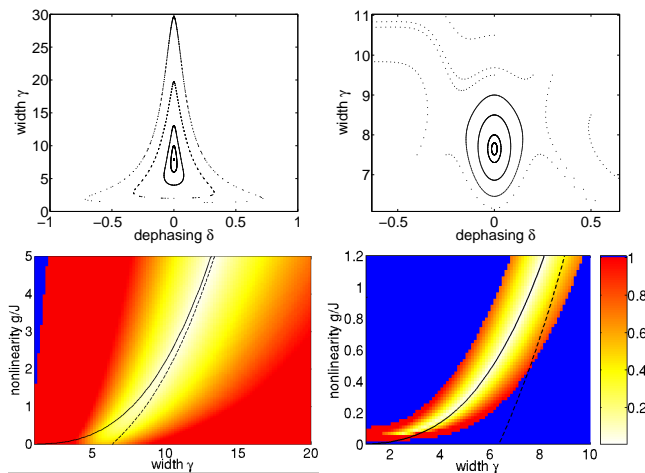


FIG. 3: Upper panels: Poincaré cross section of the effective system (5) for  $l^* = 40$  in the oscillating regime with  $l_0 = l^*/2$  (left) and the rotating regime with  $l_0 = 4l^*$  (right). The periodic orbit is located in the center of the stability island. Lower panels: The stability region of the depicted periodic orbit in the  $(\gamma, g)$ -plane. The relative deviation  $\Delta\gamma/\bar{\gamma}$  of the width  $\gamma$  averaged over the trajectory is shown in greyscale (according to the colorbar). Additionally, the solid line indicates the balance equation (8) and the broken line shows the equilibrium width of the ground state BEC in the given potential.

The above approach to the wave packet dynamics, based on the effective Hamiltonian (5), might be still oversimplified. For this reason and to check the estimate (8) we run the DNLS for different values of the nonlinearity  $g$  and harmonic confinement  $\nu$ . To reduce

the number of independent parameters we also assumed that the shape of the initial wave packet is defined by the ground state of the BEC before shifting the trap center and, hence, the wave packet width  $\gamma$  is no more an independent parameter (see the dashed line in the stability diagrams in Fig. 3). The results of this numerical studies can be summarized as follows. (i) The effect of stabilization is sensitive to the initial shift of the packet  $l_0$  relative to the position of the separatrix (3). In particular, no stabilization was observed for  $l_0 \approx l^*$ . This is actually not surprising – the separatrix is the most fragile trajectory of the pendulum and any tiny perturbation destroys it. (ii) If  $l_0$  is not in the vicinity of the separatrix, there is a finite interval of nonlinearity  $g_{\min} < g < g_{\max}$  where BEC oscillations are not decaying. (iii) The lower boundary  $g_{\min}$  is defined by the condition for appearance of a (non-negligible) stability island for the effective system (4) and is approximately given by Eq. (8). (iv) The upper boundary  $g_{\max}$  strongly depends on  $l_0$  and sometimes is not well defined in a sense that for a large  $g$  we met a temporal or incomplete stabilization. The destruction of oscillations by large nonlinearity is illustrated in the lower panels of Fig. 4 and Fig. 5. This result (taken together with the existence of the stability island) suggest, that along with the stabilization, the nonlinearity induces a different process in the system which destroys the regular oscillations of the condensate when  $g$  exceeds some critical value. A more sophisticated approach than the variational ansatz (5) is required to take this effect into account.

At this point we briefly mention the related problem of the dynamical (modulational) instability that has been studied in the context of the Bloch oscillations of a BEC of cold atoms subjected to a static force  $F$ . In particular, as shown in the recent papers [26, 27], there is

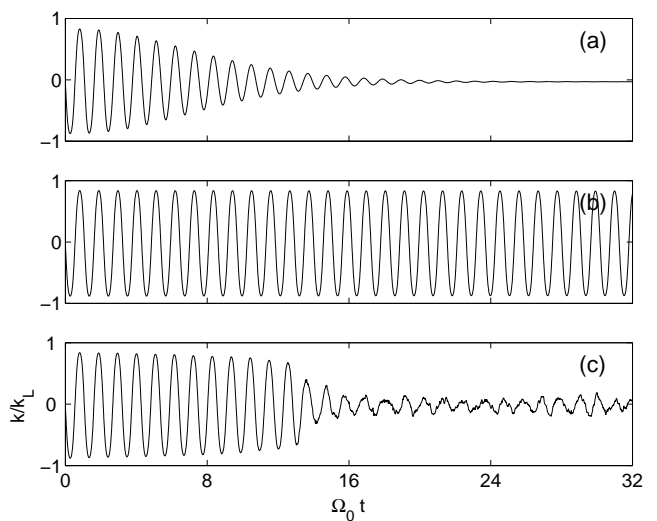


FIG. 4: Dynamics of the scaled mean atomic momentum for  $l^* = 40$ ,  $l_0 = 0.5l^* = 20$  and  $g/J = 0$  (upper panel),  $g/J = 1$  (middle panel), and  $g/J = 30$  (lower panel). The initial width of the packet is  $\gamma = 6.3, 8.5, 20.8$ , respectively.

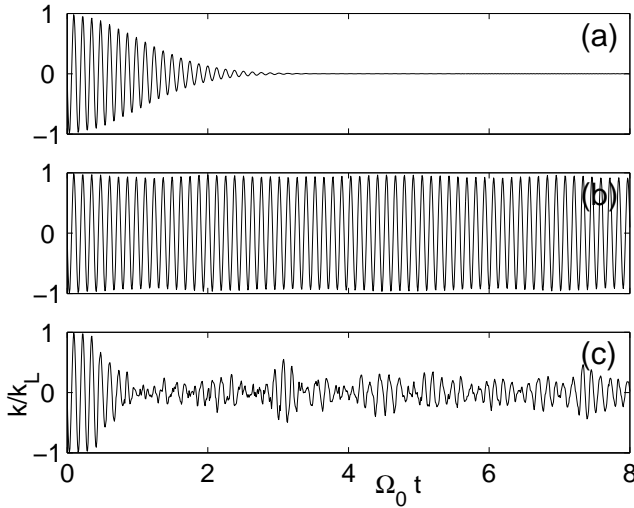


FIG. 5: Dynamics of the mean atomic momentum for  $l^* = 40$ ,  $l_0 = 4l^* = 160$  and  $g/J = 0$  (upper panel),  $g/J = 1$  (middle), and  $g/J = 5$  (lower panel). The initial width of the packet is  $\gamma = 6.3, 7.3, 12.8$ , respectively.

a critical value of the nonlinearity,  $g_{cr} \approx 3.0 dF$ , below which the Bloch oscillations are stable, while above they are unstable. Since the dynamics of the atoms in a parabolic lattice for  $l_0 \gg l^*$  can be alternatively viewed as Bloch oscillations in a static field with the local magnitude  $F = \nu l_0/d$ , a rough estimate for the expected instability regime may be drawn from this critical nonlinearity. However, an important difference between the two systems is that the modulational instability analysis

assumes a uniform state  $\gamma \rightarrow \infty$ , while in the pendulum dynamics the finiteness of  $\gamma$  is a crucial ingredient. Indeed, numerical explorations indicate that the parameter dependence is more complicated, which makes this an interesting problem for further study.

In conclusion, we have considered the 1D dynamics of a BEC of cold atoms in parabolic optical lattices. When interactions are absent, this system realizes the quantum pendulum (2) with the experimentally controllable effective Planck constant  $\hbar_{\text{eff}} = 2/l^*$ , where  $l^*$  of Eq. (3) characterizes the pendulum separatrix. The parameter  $l^*$  plays an important role both in theory and experiment. In particular, the relation between  $l^*$  and the trap center shift  $l_0 = \Delta x/d$ , used in the experiments to put the atoms in motion, defines whether BEC oscillations are symmetric with respect to the trap origin or not. The parameter  $\hbar_{\text{eff}} = 2/l^*$  also defines the rate of dephasing, because of which BEC oscillations decay even in the absence of atom-atom interactions. The effect of the latter on the discussed dynamics appears to be nontrivial. Naively, one would expect that any nonzero interaction enhances the decay of BEC oscillations. However, this is not the case – a moderate nonlinearity is found to stabilize the oscillations, which now can be described in terms of the *classical* pendulum. We believe that for  $l_0 < l^*$  this regime of BEC dynamics has been actually realized in the experiment [11], where periodic oscillations of a BEC with a frequency given by the frequency of the classical pendulum have been observed and interpreted as superfluidity. Most surprisingly, stabilization may also occur above the separatrix, which appears to not have been observed yet.

- 
- [1] J. H. Denschlag *et al.*, J. Phys. B: At. Mol. Opt. Phys. **35**, 3095 (2002).
  - [2] D. Diakonov, L. M. Jensen, C. J. Pethick, and H. Smith, Phys. Rev. A **66**, 013604 (2002).
  - [3] Biao Wu and Qian Niu, New J. of Physics **5**, 104 (2003).
  - [4] B. Wu and Q. Niu, Phys. Rev. A **61**, 023402 (2000).
  - [5] M. Jona-Lasinio *et al.*, Phys. Rev. Lett. **91**, 230406 (2003).
  - [6] K. M. Hillg  , M. K. Oberthaler, and K. P. Marzlin, Phys. Rev. A **66**, 063605 (2002).
  - [7] B. Eiermann *et al.*, Phys. Rev. Lett. **92**, 230401 (2004).
  - [8] O. Morsch, J. H. M  ller, M. Cristani, D. Ciampini, and E. Arimondo, Phys. Rev. Lett. **87**, 140402 (2001).
  - [9] R. G. Scott *et al.*, Phys. Rev. A **69**, 033605 (2004).
  - [10] G. Roati *et al.*, e-print cond-mat/0402328 (2004).
  - [11] F. S. Cataliotti *et al.*, New J. of Phys. **5**, 71.1 (2003).
  - [12] O. Morsch and M. Oberthaler, to appear in Rev. Mod. Phys. (2005).
  - [13] M. Kr  mer, L. Pitaevskii, and S. Stringari, Phys. Rev. Lett. **88**, 180404 (2002).
  - [14] M. L. Chiofalo and M. P. Tosi, J. Phys. B: At. Mol. Opt. Phys. **34**, 4551 (2001).
  - [15] A. Smerzi, A. Trombettoni, P. G. Kevrekidis, and A. R. Bishop, Phys. Rev. Lett. **89**, 170402 (2002).
  - [16] S. K. Adhikari, Eur. Phys. J. D **25**, 161 (2003).
  - [17] F. Nesi and M. Modugno, J. Phys. B: At. Mol. Opt. Phys. **37**, S101 (2004).
  - [18] Q. Thommen, V. Zehnl  , and J. C. Garreau, Phys. Rev. A **67**, 013416 (2003).
  - [19] C. Hooley and J. Quintanilla, Phys. Rev. Lett. **93**, 080404 (2004).
  - [20] A.R.Kolovsky and H.J.Korsch, International J. of Mod. Physics **18**, 1235 (2004).
  - [21] G.P.Berman, G.M.Zaslavskii and A.R.Kolovskii, Sov. Phys. JETP **54**, 272 (1981).
  - [22] A. J. Lichtenberg and M. A. Leibermann, *Regular and chaotic dynamics* (Springer, Berlin, 1983).
  - [23] A. Trombettoni and A. Smerzi, Phys. Rev. Lett. **86**, 2353 (2001).
  - [24] E. J. Heller, J. Chem. Phys. **62**, 1544 (1975).
  - [25] V. V. Konotop and M. Salerno, Phys. Rev. A **65**, 021602(R) (2002).
  - [26] Yi Zheng, M. Kostrun, and J. Javanainen, Phys. Rev. Lett. **93**, 230401 (2004).
  - [27] A. R. Kolovsky, e-print: cond-mat/0412195.